





Spontaneous symmetry breaking of substitutional solute atoms in dilute α -Ti solid solutions

Shu-Ming Chen ¹, Yang Gao,² Zi-Han Yu,^{1,3} Bi-Ning Liang,^{1,3} Shuo Cao ^{1,*}, Rui Yang ¹ and Qing-Miao Hu ^{1,†}

¹*Institute of Metal Research, Chinese Academy of Sciences, Wenhua Road 72, Shenyang 110016, China*

²*State Key Laboratory of Rolling and Automation, Northeastern University, Wenhua Road 11, Shenyang 110819, China*

³*School of Materials Science and Engineering, University of Science and Technology of China, Shenyang 110016, China*



(Received 13 December 2022; accepted 28 July 2023; published 31 August 2023)

According to classical metal physics theory, the substitutional solute atom in dilute metal solid solution occupies the high-symmetry lattice site without destroying the point group symmetry of the host lattice. However, our recent first-principles calculations showed that the substitutional solute atom Mo occupies the low-symmetry off-center position in dilute Ti solid solutions such that breaking spontaneously the point group symmetry of the hexagonal-close-packed host lattice [Q. M. Hu and R. Yang, *Acta Mater.* **197**, 91 (2020)] resulted from the Jahn-Teller splitting of the degenerated d orbitals of Mo at the Fermi level. Whether the spontaneous symmetry breaking is general for some other solid solutions and robust (e.g., to the temperature effect) remains an open question. In the present work, we investigated the site occupation of substitutional atom X in dilute Ti- X solid solution with X being all the $3d$ metal elements from V to Zn. Among the considered solute atoms, Cr, Mn, Fe, and Co are dynamically and energetically stable to occupy the low-symmetry off-center site such that the spontaneous symmetry breaking occurs, whereas V, Ni, Cu, and Zn prefer to stay at the high-symmetry lattice site. We demonstrated that the off-center occupation is robust against the supercell size adopted in the first-principles calculation and the thermal volume expansion.

DOI: [10.1103/PhysRevMaterials.7.083605](https://doi.org/10.1103/PhysRevMaterials.7.083605)

I. INTRODUCTION

As well documented in metal physics textbooks, substitutional solute atoms occupy the high-symmetry lattice sites by replacing the positions of the host atoms in metal solid solution while the point group symmetry of the host lattice remains [1]. The high-symmetry occupation has been commonsense in the field of metal physics and forms the cornerstone of the investigations of the properties of substitutional metal solid solutions.

The aforementioned commonsense about the high-symmetry lattice site occupation of substitutional solute atom was, however, recently found to be questionable for some of the metal solid solutions. The first-principles calculations of Hu and Yang [2] demonstrated that the Mo solute atom occupying the high-symmetry lattice site in α -Ti with hexagonal-close-packed (hcp) structure is dynamically unstable because it exhibits distinct imaginary vibrational frequencies. On the other hand, the low-symmetry off-center position in the basal (0001) plane (see Fig. 1) was identified to be dynamically stable for Mo to occupy, with which the point group symmetry of the hcp lattice is spontaneously broken. The lattice configuration with low-symmetry off-center occupation of Mo is about 0.13 eV more stable than the one with high-symmetry lattice site occupation of Mo. The instability of the lattice-site occupation of Mo in α -Ti was attributed to the degeneration of the d electronic orbitals of Mo at the Fermi

level of the system. Jahn-Teller splitting of the degenerated d orbitals occurs when Mo moves to the off-center position, which stabilizes the off-center occupation of Mo.

The finding of the off-center occupation of the substitutional solute atom in metal solid solution is profound because it renews our current textbook knowledge about the nature of metal solid solutions. However, there are still some open questions to be answered. First, considering the physical origin of the off-center occupation of Mo in α -Ti, Hu and Yang speculated that the off-center occupation may occur in solid solutions with Ti, Zr, and Hf as host and transition metal element in the middle of the periodic table of elements as solute to ensure sufficient d -orbital degeneration at Fermi level [2]. This speculation remains to be verified. Second, the size of the supercell used by Hu and Yang [2] is $3 \times 3 \times 2$ times the hcp unit cell. One might be concerned about whether the off-center occupation arises from the limited supercell size effect or not. Third, the off-center occupation was determined by using the 0 K first-principles calculations. A natural question would be whether it remains stable at high temperature.

To address the above questions, in the present work, we investigate the site occupation of the $3d$ element solute atoms $X = V, Cr, Mn, Fe, Co, Ni, Cu, Zn$ in α -Ti. The paper is arranged as follows. In Sec. II, we describe the methodology and calculation details of the present work. In Sec. III, we report the local lattice distortions induced by the solute atom occupying the high-symmetry lattice site and low-symmetry off-center site as well as the energy difference between the two site occupations. The thermal dynamic stability of the lattice site and off-center occupations are investigated by calculating their phonon density of states. The electronic density of states

*Corresponding author: scao14b@imr.ac.cn

†Corresponding author: qmhu@imr.ac.cn

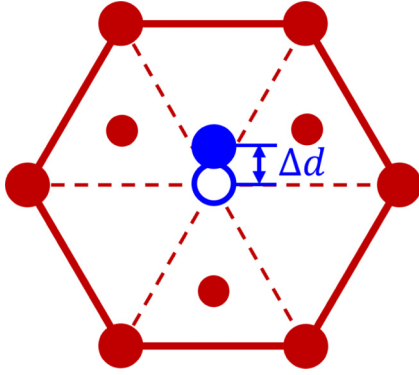


FIG. 1. Schematic representation of the off-center occupation of the solute atom Mo in hexagonal-close-packed α -Ti. The atoms are projected to the (0001) basal plane of α -Ti. The large brown solid circles represent the host Ti atoms in the (0001) basal plane while the small ones represent the Ti atoms right above and below the plane. The open blue circle represents solute atom Mo occupying the high-symmetry lattice site while the solid blue one is for the Mo atom locating at the low-symmetry off-center position in the basal plane. Δd is the in-plane distance between the high-symmetry lattice site and the low-symmetry off-center site.

is calculated to analyze the origin of the off-center occupation. The effects of supercell size and temperature on the off-center occupation are also reported in this section, taking α -Ti-Fe as a representative example. Finally, we summarize our work in Sec. IV.

II. METHODOLOGY AND CALCULATION DETAILS

We first deal with the α -Ti- X solid solution in the conventional way [3–7]. Namely, a $4 \times 4 \times 2$ supercell is constructed for pure Ti. One of the Ti atoms is then replaced by a solute atom X ; i.e., the X atom is located at the high-symmetry lattice site. The Ti- X supercells are fully relaxed by minimizing the stresses and interatomic forces. Following the geometric optimization, the dynamic stability of the relaxed Ti- X supercell is evaluated by calculating the lattice vibrational phonon density of states using the small-displacement approach, implemented as PHON by Alfè [8]. Certain atoms in the supercell are systematically shifted by a small displacement away from their equilibrium positions according to the symmetry of supercell. The resulting force matrix is then calculated by using the first-principles method. With the calculated force matrix, the phonon frequencies and phonon density of states are calculated.

In the aforementioned calculations, the geometric relaxation should not change the position of the X atom in the supercell because the total atomic force acting on X is exactly zero due to the point group symmetry of the lattice. Namely, the geometric optimization is not able to find automatically the possible low-symmetry off-center position of X . This is why the off-center occupation of the substitutional solute atom in a dilute metal solid solution has never been noticed in previous first-principles investigations [6,7]. In the present work, to determine the possible off-center position for X , the X atom in the supercell is moved slightly away from the high-symmetry lattice site [from reduced coordinate (0.50, 0.50, 0.50) to

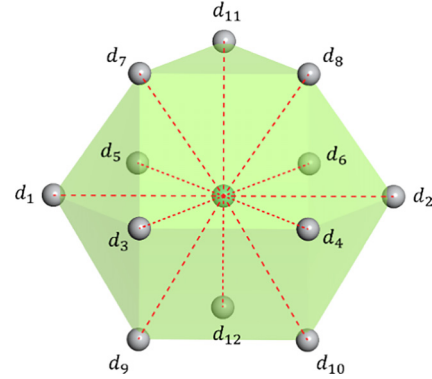


FIG. 2. Cuboctahedron depicting the next-nearest-neighbor relationship in hexagonal-close-packed structure. The distances between the atom at the center of the polyhedron and its 12 nearest neighbors are labeled with d_1 to d_{12} . For the α -Ti- X system, the solute atom X is located at the center of the polyhedron. d_1 to d_{12} are listed in Table I for the α -Ti- X systems with X occupying the high-symmetry lattice site and low-symmetry off-center site.

(0.51, 0.52, 0.50)] [9] to break the point group symmetry of the lattice. Subsequently, the supercell is fully relaxed and then its dynamic stability is checked as well.

Our first-principles calculations are performed with the first-principles plane wave method implemented in the Vienna *Ab initio* Simulation Package (VASP) [10]. The project augmented wave potential [11] is employed for the interaction between the valence electrons and ionic cores. The generalized gradient approximation parametrized by Perdew, Burke, and Ernzerhof [12] is adopted to describe the electronic exchange and correlation. The calculations are performed with non-spin-polarization because our test spin-polarized calculations demonstrated that the atoms of the magnetic elements Cr, Mn, Fe, Co, Ni do not show any magnetic moments in the dilute α -Ti- X solid solution. The plane-wave cutoff energy is set as 450 eV. A k -point mesh of $3 \times 3 \times 4$ is used to sample the Brillouin zone. The energy tolerance for the electronic minimization is set as 1×10^{-6} eV/atom and the force tolerance for the geometric optimization is set as 1×10^{-2} eV/Å. For the phonon dispersion calculations, the symmetrized force constant is calculated with atomic displacements of ± 0.015 Å.

III. RESULTS AND DISCUSSION

A. Local lattice distortions induced by lattice site and off-center solute atoms

In the present work, the local lattice distortion is characterized by the distances between X and its 12 nearest-neighbor Ti atoms, d_1 to d_{12} , as schematically depicted by the cuboctahedron in Fig. 2. d_1 to d_6 are the in-plane X -Ti distances while d_7 to d_{12} are the out-of-plane ones. The distances are listed in Table I.

As seen in Table I, for pure Ti, the in-plane X -Ti distances d_1 to d_6 are 2.934 Å while the out-of-plane distances d_7 to d_{12} are 2.875 Å, which is in perfect agreement with the experimental values, 2.951 Å and 2.894 Å respectively for the in-plane and out-of-plane distances [13]. For the high-symmetry lattice site occupation of X , the in-plane distances

TABLE I. Distances d_1 to d_{12} (see Fig. 2) between the solute atom X and its nearest-neighbor host Ti atoms in the α -Ti- X solid solution with X occupying the high-symmetry (HS) lattice site and low-symmetry (LS) off-center site. Units of Å.

	d_1, d_2		d_3, d_4		d_5, d_6		$d_7 \sim d_{10}$		d_{11}, d_{12}	
	HS	LS	HS	LS	HS	LS	HS	LS	HS	LS
Ti	2.934	2.934	2.934	2.934	2.934	2.934	2.875	2.875	2.875	2.875
Ti-V	2.898	2.896	2.898	2.917	2.898	2.888	2.839	2.843	2.839	2.838
Ti-Cr	2.886	2.974	2.886	3.124	2.866	2.633	2.809	2.735	2.809	3.010
Ti-Mn	2.904	3.070	2.904	3.154	2.904	2.500	2.766	2.664	2.766	3.187
Ti-Fe	2.913	3.034	2.913	3.362	2.913	2.414	2.753	2.683	2.753	3.206
Ti-Co	2.903	2.995	2.903	3.390	2.903	2.435	2.775	2.718	2.775	3.153
Ti-Ni	2.896	2.899	2.896	2.900	2.896	2.892	2.807	2.803	2.807	2.810
Ti-Cu	2.899	2.899	2.899	2.898	2.899	2.900	2.835	2.836	2.835	2.835
Ti-Zn	2.905	2.904	2.905	2.903	2.905	2.905	2.853	2.855	2.853	2.854

d_1 to d_6 remain identical to each other, and so do the out-of-plane distances d_7 to d_{12} for all the α -Ti- X solid solutions, with which the threefold rotation symmetry axis at the solute atom site holds.

For the solute atom $X = V, Ni, Cu,$ and Zn , the geometric optimization of the supercell with the solute atom X shifted slightly away from the high-symmetry lattice site results in a structure with the X -Ti distances deviating negligibly ($<1\%$) from their counterparts for the high-symmetry lattice site occupation of X . Practically, the X atom goes back to the high-symmetry lattice site after geometric optimization considering the accuracy of the DFT calculations. In contrast, for the solute atom $X = Cr, Mn, Fe,$ and Co , the X -Ti distances in the optimized supercell differ significantly from their counterparts for high-symmetry lattice site occupation of X , indicating a stable off-center position is found after the geometric optimization. The off-center position is still on the basal plane as seen in Fig. 1. For the low-symmetry off-center site occupation of X , the 6 in-plane distance split into 3 different values with $d_1 = d_2, d_3 = d_4, d_6 = d_7$ while the 6 out-of-plane distance split into 2 with $d_7 = d_8 = d_9 = d_{10}$ and $d_{11} = d_{12}$. The threefold rotation symmetry is broken.

To show more intuitively the X induced variation of the distances, we plot the relative distance changes for all the α -Ti- X solid solutions in Fig. 3. The relative distance change is defined as

$$\delta d_n^X = \frac{d_n^X - d_n^{Ti}}{d_n^{Ti}} \times 100 \quad (1)$$

with d_n^X and d_n^{Ti} being respectively the distances for the Ti- X and pure Ti system and $n = 1 \sim 12$ being the sequence number of the 12 nearest-neighbor Ti- X pairs, $n = 1 \sim 6$ for the in-plane pairs while $n = 7 \sim 12$ for the out-of-plane pairs (see Fig. 2).

The lattice distance changes δd_n^X are plotted in Fig. 3. For the high-symmetry lattice site occupation of X , the in-plane and out-of-plane X -Ti distances shrink simultaneously. For $X = Cr, Mn, Fe,$ and Co , the shrinkage of the out-of-plane X -Ti distance is more significant than that of the in-plane distance. The largest shrinkage is no more than 1.65% for the in-plane X -Ti distance of the Ti-Cr solid solution while it is no more than 4.25% for the out-of-plane X -Ti distance of Ti-Fe.

For the low-symmetry off-center occupation of $X = Cr, Mn, Fe,$ and Co , the in-plane X -Ti distances $d_1 = d_2$ and $d_3 = d_4$ as well as the out-of-plane distances $d_{11} = d_{12}$ expand whereas the in-plane distance $d_5 = d_6$ and out-of-plane distance $d_7 = d_8 = d_9 = d_{10}$ shrink. The variation of the X -Ti distances for the off-center occupation case is much more significant than that for the high-symmetry occupation of X . For $X = Fe$ and Co , the expansion reaches about 15% for $d_3 = d_4$ while the shrinkage reaches about 18% for $d_5 = d_6$.

In Table II, we list the in-plane distance Δd between the high-symmetry lattice site and the low-symmetry off-center site (see Fig. 1) for the α -Ti- X solid solution to show the off-center tendency of the solute atom. For $X = V, Ni, Cu,$ and Zn , Δd approaches 0, indicating that the solute atom X is still located at the high-symmetry lattice site. On the other hand, Δd is a relatively large value for $X = Cr, Mn, Fe,$ and Co . Δd increases from Cr to Mn to Fe and then decreases slightly to Co, indicating the off-center effect of the solute becomes stronger from Cr to Mn to Fe and then turns weaker to Co.

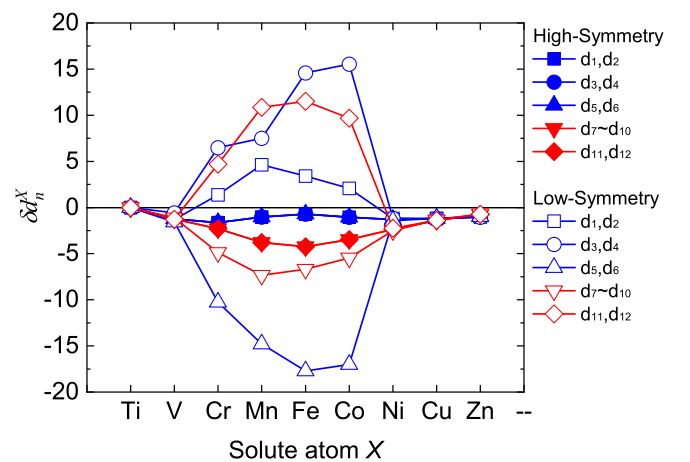


FIG. 3. Relative changes (δd_n^X) of the distances between the solute atom X and its 12 nearest-neighbor Ti atoms in α -Ti- X solid solution, as defined in Eq. (1). The solid symbols represent the distances for the system with X occupying the high-symmetry (HS) lattice site while the open ones for the system with X occupying the low-symmetry (LS) off-center site. See Fig. 2 for the notations of d_1 to d_{12} .

TABLE II. In-plane distance Δd (in Å) between the high-symmetry lattice site and the low-symmetry off-center site (see Fig. 1) for the α -Ti- X solid solution [14].

	Ti-V	Ti-Cr	Ti-Mn	Ti-Fe	Ti-Co	Ti-Ni	Ti-Cu	Ti-Zn
Δd	0.02	0.349	0.518	0.625	0.579	0.01	0.000	0.000

The distance between the solute atom and its nearest neighbors may not show directly the local strain induced by the off-center occupation. To observe more directly the local strain field induced by the solute atom occupying respectively the high-symmetry lattice site and low-symmetry off-center site, we display the Cartesian coordinate of pure Ti, Ti-Mn systems with Mn occupying the high-symmetry lattice site and low-symmetry off-center site in Fig. 4. For simplicity, here we consider solely the atoms on the basal plane where Mn is located. For Mn occupying the high-symmetry lattice site, the distance between the six in-plane nearest-neighbor Ti atoms ($Ti_1 \sim Ti_6$) of Mn and the high-symmetry lattice site is 2.904 Å compared to 2.934 Å for pure Ti (see Table II). All six in-plane nearest neighbors shift inward by about 1%. The six Ti atoms are still equivalent to each other and locate on the same circle centered with the high-symmetry lattice site. When the Mn atom moves to the low-symmetry off-center position, Ti_3 and Ti_4 shift significantly more inward whereas Ti_1 and Ti_2 shift outward. The six Ti atoms become nonequivalent to each other and do not locate on the same circle anymore.

B. Energy difference between lattice site and off-center occupations

The energy difference, $\Delta E = E_{HS} - E_{LS}$, with E_{HS} and E_{LS} being respectively the total energies of the supercells with solute atom X occupying the high-symmetry lattice site and low-symmetry off-center site, is a direct measure of the relative stability of the two site occupations of X . In Table III, we list ΔE for all the α -Ti- X systems. For $X = V, Ni, Cu,$ and Zn , ΔE is practically 0. For $X = Cr, Mn, Fe,$ and Co , ΔE increases from Cr to Mn to Fe and then decreases to Co, in accordance with the trend of Δd , which again implies the

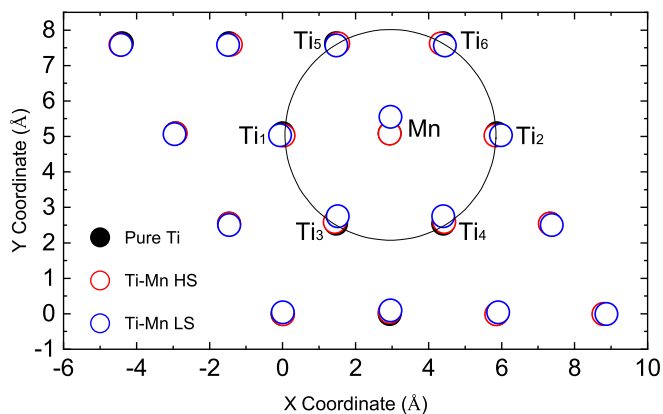


FIG. 4. Cartesian coordinates of the atoms on the basal plane where the solute atom Mn is located, showing the local strain fields of Ti with Mn occupying respectively the high-symmetry lattice site and low-symmetry off-center site.

TABLE III. Energy difference ΔE (in eV) between the configurations with X occupying the high-symmetry lattice site and the low-symmetry off-center site.

	Ti-V	Ti-Cr	Ti-Mn	Ti-Fe	Ti-Co	Ti-Ni	Ti-Cu	Ti-Zn
ΔE	0.000	0.054	0.220	0.251	0.098	0.000	0.000	0.000

off-center effect becomes stronger from Co to Mn to Fe and then turns weaker to Co.

C. Phonon dispersions for lattice site and off-center occupations

To determine the dynamic stability of the site occupation of X in α -Ti- X solid solutions, we calculate phonon dispersions of the supercells with X occupying the high-symmetry lattice site and low-symmetry off-center site. Figure 5 presents the phonon density of states (PhDOS) of α -Ti- X with X occupying the high-symmetry lattice site and low-symmetry off-center site. For $X = V, Ni, Cu,$ and Zn , no PhDOS peak appears at frequency below 0; i.e., there are no imaginary frequencies such that these solute atoms are dynamically stable to occupy the high-symmetry lattice site in α -Ti. For $X = Cr$, a PhDOS peak occurs at imaginary frequency of about -2.44 THz. For $X = Mn$ and Fe , there exist two PhDOS peaks with imaginary frequencies. For $X = Co$, one single PhDOS peak with imaginary frequency of -1.87 THz is observed. The PhDOS with imaginary frequencies demonstrates that the high-symmetry lattice site occupation is dynamically unstable for $X = Cr, Mn, Fe, Co$. When the solute atom $X = Cr, Mn, Fe, Co$ moves to the low-symmetry off-center site, all the PhDOS peaks with imaginary frequencies disappear. Namely, the low-symmetry off-center occupation of these solute atoms is dynamically stable, in agreement with the calculated lower energy of the low symmetry off-center occupation than the high-symmetry lattice site occupation of these solute atoms.

D. Electronic density of states of lattice site and off-center solute atoms

In Ref. [2] by Hu and Yang, the off-center occupation of Mo in α -Ti was attributed to the Jahn-Teller splitting of the degenerated d orbitals of Mo at Fermi level. Here we present the electronic density of states (DOS) of the solute atoms X in α -Ti to check whether the above-mentioned mechanism works for the off-center occupation of X as well. As seen in Fig. 6, the DOSs of all the solute atoms are mainly contributed by the d electrons whereas the contributions of the s and p electrons are insignificant. Therefore, we focus ourselves on the d DOS in the following part.

We first examine the partial DOS of X occupying the high-symmetry lattice site. As seen in Fig. 6(a), for $X = V$, the Fermi level locates above the bottom of the pseudogap but below the highest peak of the DOS. The d DOS at Fermi level is about 1.5 states/eV. For $X = Cr, Mn,$ and Fe , the Fermi level locates near the highest peak of the DOS. The d DOS at Fermi level is over about 3.2 states/eV. For $X = Co$, the Fermi level still locates around the DOS peak although not the highest. The d DOS at the Fermi level is about 2.8 states/eV. For $X = Ni$, the Fermi level locates above a small d DOS peak. The d DOS at Fermi level is about 1.0 states/eV. For $X = Cu$ and Zn ,

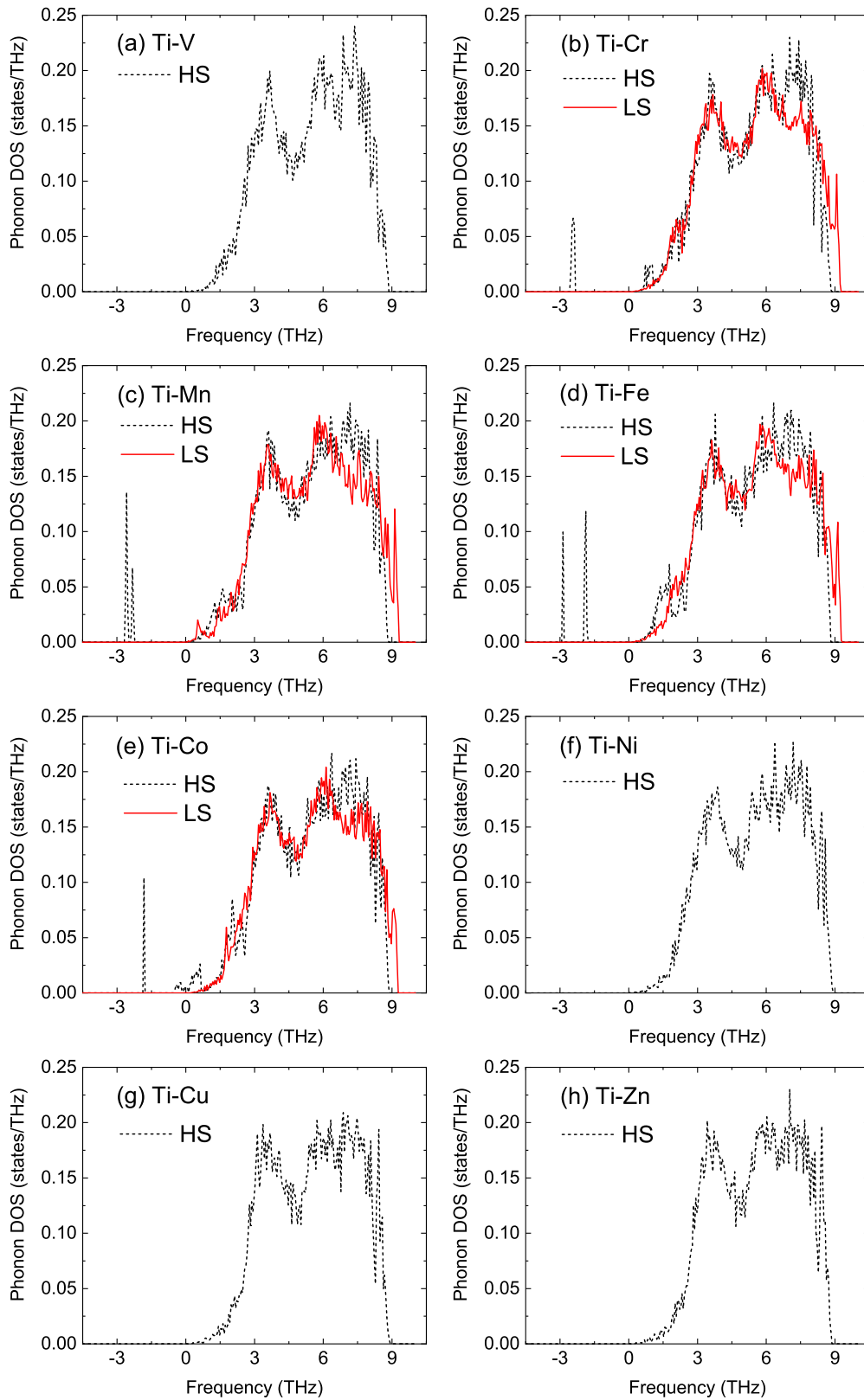


FIG. 5. Phonon density of states of the α -Ti-X systems with X occupying the high-symmetry lattice site (for all the solute atoms) and the low-symmetry off-center site (for X = Cr, Mn, Fe, Co).

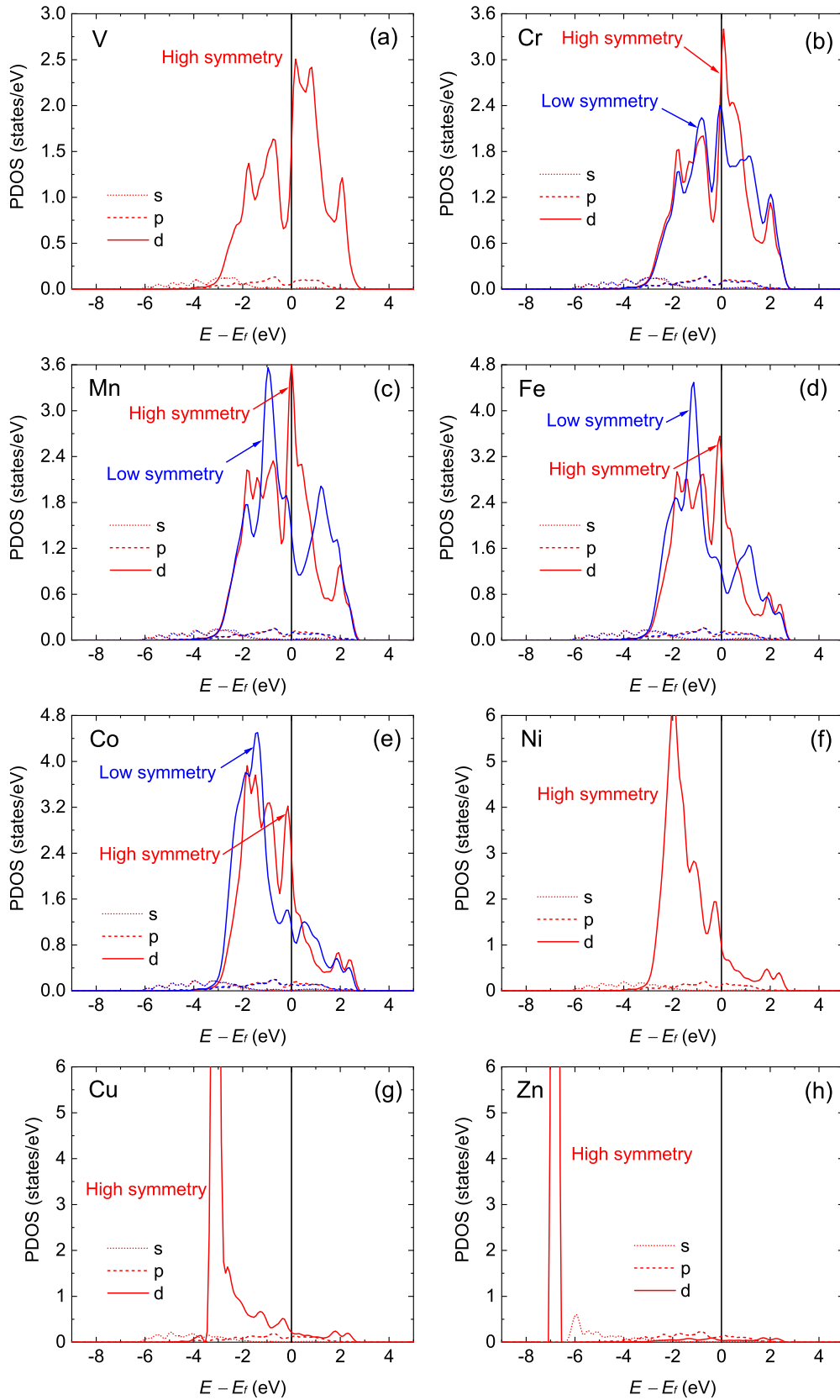


FIG. 6. Partial electronic density of states (PDOS) of solute atoms in α -Ti. The PDOS is calculated for energy from 10 eV to 15 eV with 301 data points in between. The k -point mesh is $3 \times 3 \times 4$ for the $4 \times 4 \times 2$ supercell.

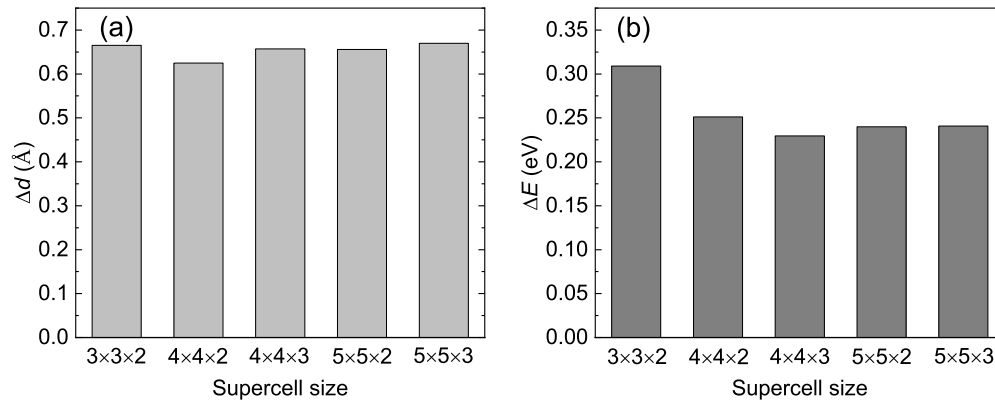


FIG. 7. In-plane distance Δd between the high-symmetry lattice-site and low-symmetry off-center site (a) and the energy difference ΔE between the two occupations (b) of α -Ti-Fe solid solution calculated with various supercell sizes.

the d DOS exhibits a very sharp peak well below the Fermi level. The d DOS at the Fermi level is very low. This is because the d orbitals are nearly fully occupied by the electrons and the d electrons are tightly bound by the atomic core.

The high d DOS peak at Fermi level for $X = \text{Cr, Mn, Fe,}$ and Co indicates that the d orbitals of these solute atoms are highly degenerated at Fermi level, which should make the α -Ti- X solid solutions with $X = \text{Cr, Mn, Fe,}$ and Co occupying the high-symmetry lattice site unstable. For $X = \text{V, Ni, Cu,}$ and Zn , the Fermi level does not sit at the d DOS peak and the d DOS at Fermi level is low. Namely, the d states are not highly degenerated at Fermi level, which is generally the electronic structure feature of a stable system. Therefore, the α -Ti- X solid solutions with $X = \text{V, Ni, Cr,}$ and Zn occupying the high-symmetry lattice site are stable.

In Figs. 6(b)–6(e), we also present the partial DOSs of Cr, Mn, Fe, Co occupying the low-symmetry off-center site in α -Ti. It is clearly seen that the d DOSs are greatly lowered as compared to those of the atoms occupying the high-symmetry lattice-site. The above features indicate that highly degenerated d states at the Fermi level for $X = \text{Cr, Mn, Fe,}$ and Co at high-symmetry lattice site split into two peaks respectively above and below Fermi level when X moves to the low-symmetry off-center site. This is the well-known Jahn-Teller splitting. With X occupying the high-symmetry lattice site, the crystal field formed by the 12 nearest neighbors of X is also highly symmetric, resulting in the degeneration of the d states of X . When X moves to the low-symmetry off-center site, the symmetry of the crystal field around the solute atom lowers accordingly, making the degenerated d states split. The Jahn-Teller splitting lowers the energy of the system and leads to a more stable off-center occupation of X than the high-symmetry lattice site occupation.

The splitting does not occur for $X = \text{V, Ni, Cu,}$ and Zn . The reason is that the d electrons of V are too fewer and insufficient to degenerate at Fermi level. For Ni, Cu, and Zn, the d electrons are too many such that the d states are well below the Fermi level and do not degenerate at Fermi level either.

The calculated DOS demonstrates that the off-center occupation originates physically from the Jahn-Teller splitting of the degenerated d orbitals of the solute atom at the Fermi level. It is noted that in concentrated solid solutions such as

high-entropy alloys (HEAs), it is usual that the atoms deviate from the perfect lattice site and induce severe lattice distortion [15–17]. This is, however, distinct from the off-center occupation of the solute atom reported in the present work. The deviation of the atoms from the perfect lattice site in HEAs is mainly ascribed to the atomic size mismatch between different atomic species where the Jahn-Teller splitting effect is not necessarily involved. The surrounding atomic environment of each atom is already highly asymmetric because its neighboring atoms are not the same. In our case for the dilute substitutional solid solution, the surrounding atoms of the solute atom are identical.

E. Supercell size effect on off-center occupation

The α -Ti-Fe solid solution is taken as a representative example to examine the supercell size effect on the off-center occupation. We construct supercells with different size, namely, $3 \times 3 \times 2$, $4 \times 4 \times 3$, $5 \times 5 \times 2$, and $5 \times 5 \times 3$ of the hcp unit cell of α -Ti. Similar to the case for the $4 \times 4 \times 2$ supercell, the crystal lattice of the supercells with Fe occupying the high-symmetry lattice site and low-symmetry off-center site are respectively determined through first-principles geometric optimization (see Sec. II). For all the supercells, the low-symmetry off-center Fe does not go back the high-symmetry lattice site, indicating that the off-center site is stable for Fe to occupy regardless of the supercell size. In Fig. 7, we present the in-plane distance Δd between the high-symmetry lattice site and low-symmetry off-center site (see Fig. 1) and the energy difference ΔE between the two occupation configurations of α -Ti-Fe solid solution calculated with various supercell size. It is clearly seen that both Δd and ΔE converge with increasing supercell size. Δd and ΔE converge respectively to about 0.66 Å and 0.24 eV, comparable to those calculated with the $4 \times 4 \times 2$ supercell, yielding Δd of 0.63 Å for Δd and ΔE of 0.25 eV. Therefore, we may conclude that the off-center occupation is indeed physical but not artificial due to the supercell size effect.

F. Effect of thermal volume expansion on off-center occupation

At finite temperature, the atoms vibrate around their equilibrium positions. For the solute atoms $X = \text{Cr, Mn, Fe,}$ and

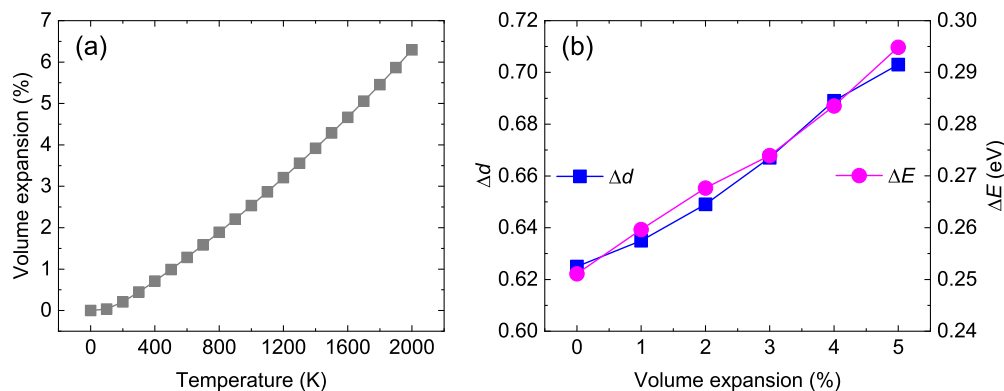


FIG. 8. Thermal volume expansion as a function of temperature for pure α -Ti (a) and in-plane distance Δd between the high-symmetry lattice site and low-symmetry off-center site as well as the energy difference ΔE between the two occupations of α -Ti-Fe solid solution as functions of the volume expansion calculated with $4 \times 4 \times 2$ supercell (b).

Co in α -Ti, the equilibrium positions are the off-center sites determined by using the static first-principles geometric optimization. The temperature-induced lattice vibration should not change directly the equilibrium positions of the solute atoms. The only factor that possibly alters the equilibrium position is the temperature-induced thermal volume expansion. To check this point, we calculate Δd and ΔE using the $4 \times 4 \times 2$ supercell of α -Ti-Fe solid solution with volume expansion up to 5%. The difference between the equilibrium volumes of the supercells with Fe occupying the high-symmetry lattice site (1101.18 \AA^3) and the low-symmetry off-center site (1101.65 \AA^3) is negligible. Therefore, we assume that the two supercells expand equally with elevating temperature when calculating ΔE .

To estimate the temperature corresponding to the volume expansion, the volume of pure α -Ti is calculated against the temperature by fitting the energy-volume data set using the thermal Birch-Murnaghan equation of state [18] within the framework of quasiharmonic approximation, as shown in Fig. 8(a). The α -Ti with hcp structure is stable at temperature below 1155 K. Above this critical temperature, α -Ti transforms to β -Ti with body-centered-cubic (bcc) structure. Namely, the temperature phase field of α -Ti is below 1155 K. The off-center occupation occurs in α -Ti. Therefore, the temperature effect should be discussed at least as high as 1155 K. As seen in Fig. 8(a), the volume expansion of α -Ti from 0 to 5% corresponds to a temperature rise from 0 K to 1700 K. Therefore, a volume expansion from 0 to 5% should cover the temperature phase field of α -Ti-Fe. Figure 8(b) displays Δd and ΔE against the volume expansion. Both Δd and ΔE increase almost linearly with increasing volume expansion, indicating that elevating temperature enhances the tendency of the off-center occupation of Fe.

G. Migration of the solute atom among equivalent off-center positions

According to the symmetry of the hcp lattice of Ti, it is easy to find that there are three equivalent off-center positions

around the high-symmetry lattice site. The off-center solute atom is expected to jump among the three equivalent positions under thermal activation. In our previous work [2], we have checked two paths for the solute atom Mo to migrate, one passing through the high-symmetry lattice site (path I) and the other going directly from one off-center site to another (path II), by using the climb image nudged elastic band (CINEB) approach [19,20]. It was shown that, for path I, the transition state for the migration is the configuration with the solute atom occupying the high-symmetry lattice site. For path II, a transition state deviating from the high-symmetry lattice site was identified. Such transition state is also threefold degenerated according to the symmetry of the hcp lattices. The off-center positions and the transition states are schematically displayed in Fig. 9.

In this work, we optimize the transition states of path I and path II determined in Ref. [2] for Ti-X ($X = \text{Cr, Mn, Fe, and Co}$), with which the energy barriers for the migration of the off-center solute atoms are listed in Table IV. It is shown that, for Ti-Cr, Ti-Mn, and Ti-Fe, the migration energy

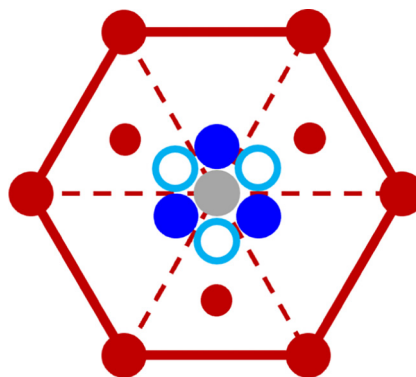


FIG. 9. Schematic representation of the high-symmetry lattice site (gray circle), off-center positions (blue circles), and transition states (open cyan circles) in α -Ti with hexagonal-close-packed structure. The positions are projected to the (0001) basal plane of α -Ti.

TABLE IV. Energy barrier (in eV) for the migration of the solute atom among the three equivalent off-center positions. The migration path I passes through the high-symmetry lattice site while path II goes directly from one off-center site to another.

	Ti-Cr	Ti-Mn	Ti-Fe	Ti-Co
Path I	0.054	0.220	0.251	0.098
Path II	0.021	0.158	0.217	0.098

barrier for path I is higher than that for path II. For Ti-Co, the migration energy barriers for path I and path II are identical. The reason is that the transition state for path II ends up with the high-symmetry lattice site occupation configuration (transition state of path I) automatically after the geometric optimization for Ti-Co.

The calculated migration energy barrier allows us to estimate roughly the jump frequency of the solute atom in between the off-center positions. A migration energy barrier of ΔE_b generates a success probability of $f = e^{-\frac{\Delta E_b}{k_B T}}$ for the solute atom jumping from one off-center position to another, with k_B being the Boltzmann constant and T the temperature. According to the transition state theory, the attempt frequency ν for the jump may be taken roughly as the thermal vibrational frequency (about several THz). Therefore, the jumping frequency of the off-center solute atom is $f\nu$. Taking Ti-Fe as an example, the jumping frequency is at the magnitude of about 10^8 Hz at temperature of 300 K. Because the migration energy barriers for Cr, Mn, and Co are lower than that for Fe, the jumping frequencies of these solute atoms are even higher than that of Fe. This means that, at room temperature, the solute atom jumps very frequently among the three off-center positions. It is noted that the energy barrier for Cr is as low as 0.021 eV. Therefore, Cr may tunnel the energy barrier through quantum effect and evolve to different equivalent low-symmetry sites without the help of the thermal activation, which will average-out of the symmetry breaking.

IV. SUMMARY

In the present work, we investigated the site-occupation of the 3d metal element substitutional solute atom in α -Ti solid solution using first-principles calculations. The main results are summarized as follows.

(1) The solute atom $X = \text{V, Ni, Cu, Zn}$ is dynamically and energetically stable to occupy the high-symmetry lattice site whereas $X = \text{Cr, Mn, Fe, Co}$ prefers to occupy the low-symmetry off-center site away from the lattice site. The latter solute atoms break spontaneously the point group symmetry of the host lattice.

(2) The off-center occupation originates from the Jahn-Teller splitting of the degenerated d states of the solute atom at Fermi level.

(3) The off-center occupation is robust against the supercell size adopted in the calculations and thermal volume expansion. Elevating temperature enhances the tendency of the off-center occupation.

(4) At finite temperature, the off-center solute atom jumps frequently among three equivalent off-center positions around the high-symmetry lattice site. The solute atom such as Cr with quite low energy barrier between the equivalent low-symmetry configurations may tunnel the energy barrier through quantum effect and evolve to different low-symmetry sites without the help of the thermal activation, which will average-out of the symmetry breaking.

ACKNOWLEDGMENTS

We are very grateful to Prof. Xinzhen Li and Dr. Yuchen Zhu from Beijing University for the discussions about quantum tunneling. This work is financially supported by the National Natural Science Foundation of China under Grants No. 91860107, No. 52071315, No. 52001307, and No. U2106215, the National Science and Technology Major Project under Grant No. J2019-VI-0012-0126, and the National Key Research and Development Program of China under Grant No. 2021YFC2801803.

-
- [1] D. Feng, *Metal Physics, Vol. I, Structure and Defects* (Science Press, 1998).
- [2] Q. M. Hu and R. Yang, *Acta Mater.* **197**, 91 (2020).
- [3] T. Uesugi and K. Higashi, *Comput. Mater. Sci.* **67**, 1 (2013).
- [4] T. Wang, L. Q. Chen, and Z. K. Liu, *Metall. Mater. Trans. A* **38**, 562 (2007).
- [5] P. Salo, K. Kokko, R. Laihia, and K. Mansikka, *J. Phys.: Condens. Matter* **7**, 2461 (1995).
- [6] L. F. Huang, B. Grabowski, J. Zhang, M. J. Lai, C. C. Tasan, S. Sandlöbes, D. Raabe, and J. Neugebauer, *Acta Mater.* **113**, 311 (2016).
- [7] C. Zou, J. Li, W. Y. Wang, Y. Zhang, B. Tang, H. Wang, D. Lin, J. Wang, H. Kou, and D. Xu, *Comput. Mater. Sci.* **152**, 169 (2018).
- [8] D. Alfè, *Comput. Phys. Commun.* **180**, 2622 (2009).
- [9] Our test calculations on the Ti-Mn system showed that the Mn atom shifted along all a , b , and c directions, e.g., with reduced coordinates (0.52, 0.54, 0.52), will go back the basal plane after the geometric optimization. Therefore, we put all other solute atoms on the basal plane by setting the initial reduced coordinates as (0.51, 0.52, 0.50).
- [10] G. Kresse and J. Furthmüller, *Comput. Mater. Sci.* **6**, 15 (1996).
- [11] P. E. Blöchl, *Phys. Rev. B* **50**, 17953 (1994).
- [12] J. P. Perdew, K. Burke, and M. Ernzerhof, *Phys. Rev. Lett.* **77**, 3865 (1996).
- [13] R. M. Wood, *Proc. Phys. Soc.* **80**, 783 (1962).
- [14] S. Cao, S. Z. Zhang, J. R. Liu, S. J. Li, T. Sun, J. P. Li, Y. Gao, R. Yang, and Q. M. Hu, *Comput. Mater. Sci.* **197**, 110620 (2021). The in-plane distances listed in Table 1 of this reference, calculated with a $4 \times 4 \times 3$ supercell, were taken as half of the real values by mistake.
- [15] Y. Zhang, Y. N. Osetsky, and W. J. Weber, *Chem. Rev.* **122**, 789 (2021).
- [16] Q. He and Y. Yang, *Front. Mater.* **5**, 42 (2018).

- [17] H. Song, F. Tian, Q. M. Hu, L. Vitos, Y. Wang, J. Shen, and N. Chen, *Phys. Rev. Mater.* **1**, 023404 (2017).
- [18] A. Otero-de-la-Roza, D. Abbasi-Pórez, and V. Luña, *Comput. Phys. Commun.* **182**, 2232 (2011).
- [19] G. Henkelman, B. P. Uberuaga, and H. Jónsson, *J. Chem. Phys.* **113**, 9901 (2000).
- [20] G. Henkelman and H. Jónsson, *J. Chem. Phys.* **113**, 9978 (2000).